

PROGRESS IN SEMI-EMPIRICAL MODELLING OF MAIN-SEQUENCE STELLAR CHROMOSPHERES

E.R. HOUDEBINE

Space Science Department, ESA-ESTEC

Postbus 299, 2200 AG Noordwijk, The Netherlands

Abstract. We present the results of a long term research programme on the outer atmospheres of main-sequence dwarfs. Combining NLTE-radiation transfer calculations with high resolution spectroscopic observations have led to significant progress in understanding chromospheric physical properties and spectral signatures. We emphasize that in order to unravel the extremely complex physics of the outer atmosphere and its energy source, magnetic field and acoustic wave dissipation, one must isolate the influence of all stellar parameters.

1. Introduction

In main-sequence dwarfs, the chromosphere is the prime signature of two important stellar phenomena: acoustic waves that dissipate in the atmosphere and the dynamo mechanism that generates the magnetic field. Little is understood about the former and near to nothing for the latter. In both cases theoretical calculations are difficult, but in fact extremely little is also known from observations. The reason for this is rather simple; acoustic heating is often masked by magnetic variability, hence difficult to observe, and the signatures of the dynamo mechanism are dependent on numerous stellar parameters. However, that complexity which has been a barrier to progress for decades is not insurmountable providing that one can isolate the effects of the stellar parameters involved.

One must realize that it is *necessary to investigate stellar chromospheres and understand their physics* in order to constrain the magnetic dynamo. Why chromospheres? For the very simple reason that variability can be observed to its lowest levels, unlike at X-ray or UV wavelengths. In order to understand the formation of the chromospheric spectral signatures that one

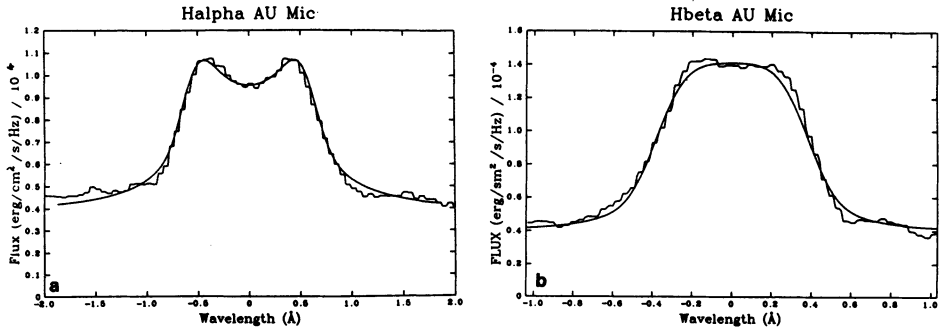


Figure 1. Observed and theoretical H_{α} and H_{β} profiles for AU Mic (from Houdebine, 1990, 1991 and Houdebine & Doyle 1994a)

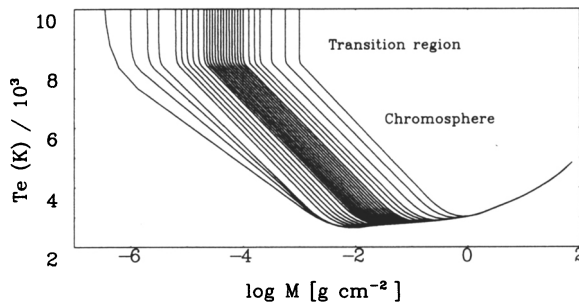


Figure 2. Grid of model chromospheres for M1/2 dwarfs. This grid covers the entire range in magnetic activity level, from basal to the highest pressure atmospheres

uses as probes to magnetic activity, we have to use NLTE-radiation transfer calculations. Recently, we made another step in this direction: we developed the first grid of model chromospheres that can reproduce observations for a wide range of parameter values for the M1/2 dwarfs.

2. Method

It is no simple matter to investigate the physical characteristics of the chromosphere because of its non-LTE and dynamic properties and the optically thick character of its spectral diagnostics. Therefore, as mentioned above, one must use complex NLTE-radiation transfer methods. We preferred the semi-empirical approach because of its efficiency and because too little is known about non-thermal heating mechanisms that are necessary for the immediately competing “*ab initio*” approach (e.g. Mullan & Cheng 1994, Rammacher & Ulmschneider 1992). This however understates important approximations such as surface inhomogeneities for instance.

The final outcome of this modelling should be a multi-dimensional grid of model atmospheres that investigates as many stellar variables as possible

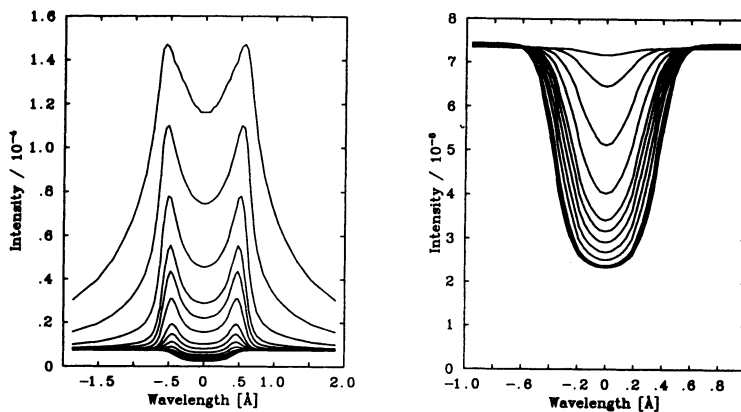


Figure 3. H_{α} profiles for the M1/2 grid of model atmospheres shown in Fig. 2. The arrow shows the variations in the profile when the level in activity diminishes

and that can reproduce most observed spectral features in their shapes and empirical correlations. To achieve this, one must almost inevitably observe the following steps:

- [1] Model to some accuracy the chromospheres of a few stars that will be used as *reference points* in the domain to be investigated.
- [2] Extrapolate the models into a denser grid of model atmospheres.
- [3] Test the models against a large set of observations.

We have applied this procedure to the “magnetic activity parameter” in M1/2 type dwarfs ($(R-I)_K=0.87$), and describe our main results below.

3. High activity dwarfs and low activity dwarfs

Our first study focused on the relevance of numerical and physical approximations to modelling M dwarf atmospheres (Houdebine & Panagi 1990). It was shown for instance that; a rather complete model atom was required to model the hydrogen lines that are an essential spectral diagnostic to stellar chromospheres.

We pursued by modelling in detail the hydrogen spectrum of AU Mic (dM1e) (Houdebine 1990, 1991, Houdebine & Doyle 1994a, b). We investigated within a restricted range the effects of a few stellar (T_{eff} , $v \sin i$) and atmospheric parameters (turbulence, temperature structure) that were necessary for the detailed modelling. We showed that a very thin transition region was required to account for the observed Ly_{α} to H_{α} surface flux ratio. Then, to reproduce the H_{α} and H_{β} profiles (Fig. 1) we put forward a complete set of constraints on the possible chromospheric structures from 5,000 K to 50,000 K (e.g. transition region column mass at $\log(M) \sim -3$). As previous investigations on the dMe chromospheric modelling, our study

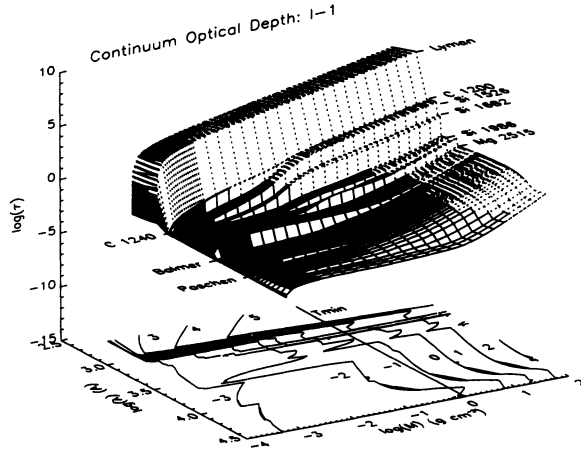


Figure 4. Continuum optical depth as a function of wavelength and column mass for a high pressure M dwarf atmosphere (from Houdebine et al. 1995a)

is evidence that high electron density and collisional control is a necessary condition to drive the Balmer lines into emission.

We also studied four low activity dM stars that were observed spectroscopically in the optical and ultraviolet regions (Houdebine & Doyle 1994d, Doyle et al. 1994). We reproduced the observed Ca II H & K fluxes and $H\alpha$ equivalent widths with a range of low pressure/low temperature minimum model atmospheres.

4. Grids of model atmospheres

4.1. MAGNETIC ACTIVITY: THE HYDROGEN AND CALCIUM LINES

Based on the previous constraints on respectively high and low activity chromospheres, we extrapolated four grids of model atmospheres with the temperature minimum either at 2,660 K or 3,000 K (Houdebine et al. 1995a). More than one grid was used in order to further test the effects of some chromospheric parameters, and englobe the possible domain of chromospheric properties. Later, these grids were merged into a unique grid of models (Fig. 2) that was refined by comparison to a large set of observations (see § 5).

We found that when decreasing the transition region pressure (i.e. the chromospheric temperature gradient), the Balmer lines change rapidly from emission to strong absorption, then the profiles weaken and become narrower until they disappear totally (zero $H\alpha$ stars). All hydrogen series, except the Lyman series for intermediate and high pressures, are sensitive to the temperature minimum when large changes are considered.

Our grids of models can successfully reproduce all types of observed H_{α} profiles (Fig. 3) : (i) high activity with strong emission and weak self-reversal, (ii) filled in intermediate activity with inner wings in emission and the core in absorption, (iii) intermediate activity with strong and broad absorption, (iv) low activity with weak and narrow absorption.

TABLE 1: Radiative losses ($10^6 \text{ erg cm}^{-2} \text{ s}^{-1}$) in various spectral bands: X-rays, EUV, UV spectral lines from IUE (F_{UV}), Mg II and Ca II lines, H I Balmer lines, the sum in H I series, continuum in the 50-5000nm range. In the second column we specify whether the source is observational or theoretical. We show in parentheses the percentage to the total radiative losses. We also give the ratio of the radiative losses of non-thermal origin (L_{NT}) to the bolometric luminosity (from Houdebine et al. 1995a)

Name	AX Mic	BY Dra	AU Mic	EQ Peg	YZ CMi	Prox Cen
Spectral type	M1	K7	M2	M4+M5.5	M4.5	M5
F_X	0.09 (0.3)	6.3 (4.6)	15.0 (12.1)	4.2 (4.8)	4.1 (3.3)	0.6 (0.7)
F_{EUV}	0.4 (1.2)	34 (25.0)	10.5 (8.4)	4.5 (5.1)	26 (20.8)	2.7 (3.3)
F_{UV}	0.26 (0.8)	4.9 (3.6)	2.4 (1.9)	1.7 (1.9)	3.8 (3.0)	0.4 (0.5)
Mg	0.24 (0.7)	2.9 (2.1)	0.89 (0.7)	2.0 (2.3)	0.85 (0.7)	0.06 (0.07)
Ca	0.11 (0.3)	0.31 (0.2)	1.5 (1.2)	1.5 (1.7)	0.55 (0.4)	0.063 (0.07)
H Balmer	-0.49 (-1.5)	3.58 (2.6)	4.5 (3.6)	1.71 (1.9)	3.9 (3.1)	2.4 (3.0)
H $_{tot}$	-0.18 (-0.5)	7.01 (5.2)	8.55 (6.9)	3.94 (4.5)	7.05 (5.6)	5.05 (6.3)
UV Cont.	32.8 (97)	80.7 (59.3)	85.5 (68.8)	70.0 (79.7)	82.8 (66.1)	74.6 (92.3)
Total	33.7	136.1	124.3	87.8	125.2	80.8
L_{NT}/L_{Bol} (%)	1.0	0.4	0.9	1.0	2.3	1.4

4.2. MAGNETIC ACTIVITY: THE UV CONTINUUM

With the above grids, we investigated the formation of the continuum intensity from 50nm to 5000nm (Houdebine et al. 1995a, Fig. 4). We showed that the UV intensity is most dependent on the transition region pressure, although the temperature minimum also plays an important role. We examined the formation of the continuum and pointed out that, although large differences appear for very low or very high activity levels, in general the global picture is much alike the Sun. These models allowed to predict a significant UV excess due to the chromospheric emission, that we later detected in broad band photometry.

An important conclusion obtained in this study is that for active dMe stars, the chromosphere becomes such an efficient radiator in the continuum that it largely dominates the total radiative budget (Table 1). This may contribute to the observed apparent “saturation” in spectral line surface fluxes, which in turn may therefore not be relevant to a saturation in magnetic activity level.

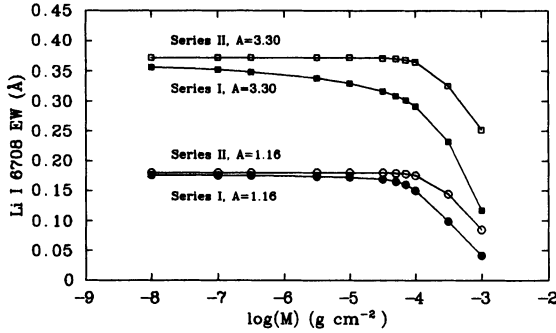


Figure 5. Effect of magnetic activity on the Lithium 6708 Å equivalent width. Photospheric lines are sensitive to magnetic activity (from Houdebine & Doyle 1995)

Further comparison to pre-main sequence model atmospheres and observations highlighted the continuity with main-sequence stellar activity. They also showed that there is almost undoubtedly a chromospheric contribution to $H\alpha$ and the blue/UV excess for pre-main sequence stars.

4.3. MAGNETIC ACTIVITY: PHOTOSPHERIC LINES, THE LITHIUM EXAMPLE

So as to gauge the effect of magnetic activity on “normal photospheric lines”, we investigated the influence of the chromosphere on the Li I lines with the same grids of models. We carried out this study because the Li I 6708 Å line is often used as an age indicator (e.g. Pinsonneault 1994 for a review), and because the chromospheric contribution of numerous photospheric lines may contribute to the total radiative budget.

We show that the Lithium lines are in fact activity sensitive and that this dependence commences at rather high activity levels, i.e. when $H\alpha$ fills in (Fig. 5). As in the solar case, this chromospheric plage effect weakens the line equivalent widths and may cancel the photospheric spot effect on disc integrated measurements. Changes in the line profiles and equivalent widths are due to the non-photospheric UV continuum that further ionises neutral lithium and depletes the line optical depths, whereas in solar plagues collisional ionisation is the driving mechanism. We concluded that in K dwarfs, both mechanisms would compete to yield a similar effect.

4.4. EFFECTIVE TEMPERATURE: THE HYDROGEN AND CALCIUM LINES

In dMe stars, hydrogen and Ca II lines are collisionally controlled. In solar-type stars, this only applies to the Ca II lines. In order to investigate the

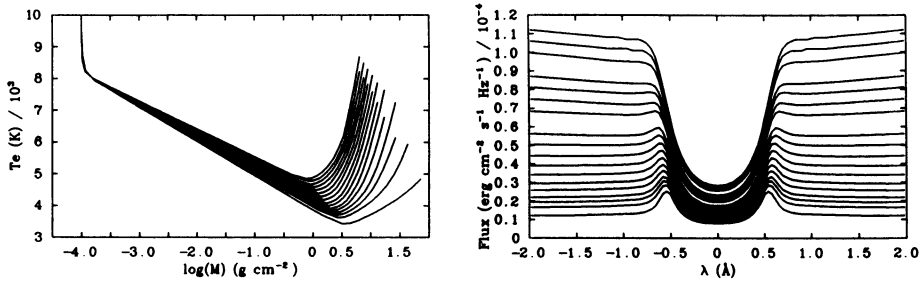


Figure 6. Grid of model atmospheres to investigate the effect of effective temperature (from G to M dwarfs) on the line formation; e.g. H_α

importance of the photospheric radiation field on the line profiles and their formation, we created another grid of model atmospheres suited to that purpose. Our results allowed us to study the complex interplay of collisional and radiative processes from G0 to M4 dwarfs (Houdebine & Doyle 1994c). In particular it shows clearly the progressive change from radiative to collisional control of the H_α line formation. It also emphasizes the importance of the contrast effect in M dwarfs, i.e., for a given transition region pressure, the H_α line changes from absorption in G dwarfs to emission in M dwarfs (Fig. 6).

5. Comparison to observations

We compared our calculations for dM1/2 chromospheres to high resolution observations for a selected sample of stars in a narrow spectral range ($(R-I)_K = 0.875 \pm 0.05$) (Houdebine et al. 1995b, c). For the first time, we bring evidence that grids of uniform model atmospheres in the plane-parallel and hydrostatic equilibrium approximations can reproduce the average chromospheric spectral signatures throughout the entire activity range (e.g. Fig. 7). We confirmed our numerical prediction that when magnetic activity level rises, the H_α line is first weak, increases in absorption strength, fills in and eventually goes into emission. We obtained a correlation between the H_α line width and equivalent width that is in good agreement with our model calculations. We show that intermediate activity stars (filled in profiles), a previously unknown group, represent a significant proportion of the stellar population. On the other hand, we find an exclusion zone in the $[0.25\text{\AA}; -1\text{\AA}]$ domain, that finds a simple explanation in the rapid change over from the absorption to the emission regimes.

We found no “zero- H_α ” stars but instead an H_α basal equivalent width of $\sim 0.20\text{\AA}$ which with reference to our models points to a transition region column mass of $\log(M) \sim -5.5$, very close to the solar value. This implies that the vast majority of M1 type dwarfs are much more active than the

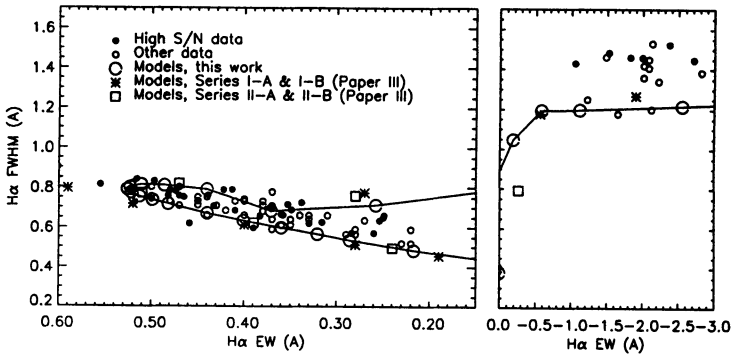


Figure 7. $H\alpha$ FWHM against its equivalent width for observations and models. The left and right panels are respectively for absorption and emission profiles. When the activity level increases, the equivalent width first increases in absorption, reaches a maximum, then decreases as the profile “fills in” and eventually goes into emission (from Houdebine et al. 1995c)

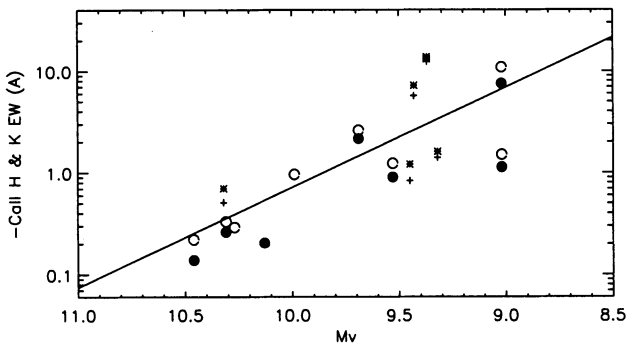


Figure 8. Ca II line equivalent widths as a function of absolute visual magnitude. This is a forceful indication that in average the stellar magnetic flux grows as the power of 6.5 of the stellar radius: a decisive constraint for stellar dynamo and atmosphere theories

Sun (per unit area). At the other end, a maximum $H\alpha$ equivalent width of $\sim 0.52\text{\AA}$ was observed which agrees with our calculations. In general, we showed that discrepancies between models and observations are evidence for surface inhomogeneities and temporal variability, even for the less active dM stars.

We found that the equivalent widths in the H and K lines are tightly correlated, and the line formation tends towards the optically thin and thick regimes respectively at low and high activity levels. We confirmed a near UV excess in active dwarfs (dMes) that increases with activity level; typically ~ 0.1 magnitudes in U-B. It is three times larger than expected from our calculations which again emphasizes the importance of the UV continuum in the radiative budget.

A more detailed investigation of the luminosity effect confirms that

dMe's are more luminous than their less active absorption line counterparts, which we interpret as an indication that active dwarfs may not have yet reached the main sequence and may form an intermediate class between T Tauri stars and main sequence stars.

The chromospheric pressures inferred from H α observations (Houdebine et al. 1995) are higher than expected if the chromosphere was heated solely by acoustic waves (Mullan & Cheng 1994), and thus the Ca II line fluxes relate to magnetic activity. We found that these fluxes rise as the power of 4.54 of the stellar radius (Fig. 8), and hence the stellar magnetic flux is expected to rise as the power of 6.54 of the radius. This correlation is also found in H α though with a larger scatter because of the more complex variations in this line as a function of activity level.

To conclude, our studies show that NLTE-radiation transfer modelling of stellar chromospheres is a fundamental key to progress in our understanding of magnetic and acoustic heating. It provides an essential information on the physical properties of the outer atmosphere and the behaviour of the spectral features. They yield abundant predictions that can be easily tested with spectroscopic observations. We proved that through a careful selection work, one can isolate the effects of the stellar parameters and therefore make substantial progress.

References

- Doyle, J.G., Houdebine, E.R., Mathioudakis, M. & Panagi, P.M. 1994, *A&A* 289, 233
Houdebine, E.R. 1990, PhD Dissertation of Paris XI University-Orsay
Houdebine, E.R. 1991, *Mechanisms of Chromospheric and Coronal Heating*, eds. P. Ulmschneider, E.R. Priest & R. Rosner, 182
Houdebine, E.R. & Panagi, P.M. 1990, *A&A* 231, 459
Houdebine, E.R. & Doyle, J.G. 1994a, *A&A* 289, 169 (Paper I)
Houdebine, E.R. & Doyle, J.G. 1994b, *A&A* 289, 185 (Paper II)
Houdebine, E.R. & Doyle, J.G. 1994c, *Cool Stars, Stellar Systems and the Sun*, ed. J.P. Caillault, ASPCS 64, 423
Houdebine, E.R. & Doyle, J.G. 1994d, *Cool Stars, Stellar Systems and the Sun*, ed. J.P. Caillault, ASPCS 64, 420
Houdebine, E.R. & Doyle, J.G. 1995, *A&A*, in press (Paper IV)
Houdebine, E.R., Doyle, J.G. & Kościelicki, M. 1995a, *A&A* 294, 773 (Paper III)
Houdebine, E.R., Mathioudakis, M., Doyle, J.G. & Foing, B.F. 1995b, *A&A* in press (Paper V)
Houdebine, E.R., Foing, B.H. & Doyle, J.G. 1995c, *A&A* submitted (Paper VI)
Mullan, D.J. & Cheng, Q.Q. 1994, *ApJ* 435, 435
Pinsonneault, M.H. 1994, *Cool Stars, Stellar Systems and the Sun*, ed. J.P. Caillault, ASPCS 64, 254
Rammacher, W. & Ulmschneider, P. 1992, *A&A* 253, 586
Wilson, O.C. & Bappu, M.K.V. 1957, *ApJ* 125, 661